

Title

Micro-Martingale and Integral Take-Profit: A Dynamic Multi-Pair Framework for Volatility-Adaptive Trading in Cryptocurrency Markets

Author

Li-Yung Chen

Department of Surgery, Gangshan Branch, Kaohsiung Armed Forces General Hospital, Kaohsiung 820, Taiwan

Abstract

This study introduces a volatility-adaptive Martingale-derived trading framework that integrates three structural innovations: **Micro-Martingale decomposition**, **Integral Take-Profit**, and a **nonlinear reverse-pair hedging mechanism** based on the USDT/DOGE inverse perpetual swap. Traditional Martingale systems fail due to fixed spacing, exponential position scaling, and sensitivity to directional trends. In contrast, the proposed architecture subdivides each entry layer into differential micro-positions, enabling smooth exposure distribution; harvests fragmented rebounds through a weighted integral exit mechanism; and stabilizes drawdowns through the convex expansion of the inverse-price function $y = 1/x$.

Using real execution data from 2023–2025 across DOGE/USDT, LTC/USDT, and USDT/DOGE, we evaluated profitability, holding duration, position geometry, and cross-pair interactions. Despite multiple high-volatility market regimes—including the severe **2024-08-05 deleveraging event** and the **policy-driven downturn in early 2025**—the system produced a **monotonically increasing profit curve**, with win rates exceeding 98% and median holding times under three hours. DOGE and LTC served as forward volatility-harvesting modules, while the reverse-pair UD layer expanded during downtrends and accumulated funding-fee yield, functioning as a convex “insurance-miner” within the strategy cluster.

Overall, the three-module architecture operated as a **self-correcting, volatility-**

responsive engine, demonstrating that Martingale-derived systems—when redesigned with adaptive micro-scaling and inverse-pair hedging—can transition from fragile doubling schemes into **robust, crash-resilient quantitative strategies** suitable for highly stochastic cryptocurrency markets.

1. Introduction

Cryptocurrency markets exhibit several structural properties that fundamentally differentiate them from traditional financial systems. These include extreme intraday volatility^[^1], deep liquidity in perpetual futures markets^[^2], and nonlinear price microstructure dynamics^[^3]. These characteristics often cause classical portfolio frameworks to misestimate risk. Models designed for equities or foreign exchange markets frequently fail to account for the convexity, microstructure noise, and funding-driven distortions inherent to cryptocurrency assets^{[^4][^5]}.

For example, the Martingale strategy has long been criticized for its reliance on exponential position growth, rigid spacing assumptions, and a fragile dependence on full mean reversion^{[^6][^7]}. In cryptocurrency markets, these limitations become even more severe. Rapid downward shocks and structurally unpredictable drawdowns frequently overwhelm fixed grid spacing, causing geometrically expanding positions to collide with margin constraints. In a leveraged environment, this dynamic exposes classical Martingale systems to abrupt liquidation risk, often long before any mean-reversion can materialize.

From a practical standpoint, the motivation for this study came from a recurring operational challenge. Traditional Martingale variants consistently failed to survive large, abrupt cryptocurrency-market drawdowns, even when implemented conservatively. These failures were not due to execution errors, but reflected a fundamental mismatch between classical Martingale assumptions and the volatility profile of cryptocurrency assets. This mismatch raises a broader question for both practitioners and researchers. Can Martingale logic be re-engineered—rather than abandoned—to function within a market

microstructure fundamentally different from traditional assets?

To explore this question, three representative instruments were selected: Asset-A/USDT (forward pair), Asset-B/USDT (mid-range stabilizer), and the reciprocal USDT/Asset-A reverse pair. These assets were chosen because they demonstrated consistent oscillatory behavior and recoverability after major dislocations (2022–2025). They also offered price granularity compatible with micro-position decomposition. In contrast, instruments with extremely high prices or highly unstable volatility were excluded, as those conditions were incompatible with the fine-grained differential scaling required by the framework.

Paradoxically, the very structural conditions that undermine traditional Martingale systems also introduce advantages unique to cryptocurrency markets. Unlike traditional assets, cryptocurrency markets offer instruments with unique behaviors. For example, perpetual swaps generate continuous funding flows^[^8] and exhibit dense, high-frequency bid–ask oscillations^[^9]. Moreover, crypto markets include inverse-quoted pairs such as USDT/Asset-A, whose price geometry follows a convex $1/x$ mapping^[^10]. Because the stablecoin side of the pair remains effectively anchored near unity, the inverse pair’s price curve exhibits asymmetric convexity not available in fiat–fiat currency markets. Together, these conditions create frequent micro-reversion windows and provide a mathematically favorable environment for reconstructing Martingale logic as a volatility-adaptive mechanism.

Guided by these observations, this study introduces a redesigned framework to address the practical limitations of classical Martingale systems. The framework comprises three core innovations:

1. Micro-Martingale Decomposition: This technique fractionalizes each layer into multiple micro positions, converting geometric progression into a quasi-continuous exposure surface and suppressing runaway convexity — a primary failure mode of traditional Martingale designs^[^11].
2. Integral Take-Profit Mechanism: This mechanism does not remove the requirement that price must exceed the position’s cost basis to realize profit. Instead, it continuously lowers the effective cost basis through

micro-position decomposition and downward repositioning during drawdowns. Even modest rebounds are sufficient to surpass the updated cost basis and trigger profit realization.

3. Reverse Pair Hedging: The framework incorporates hedging with the inverse pair (USDT/Asset-A), exploiting inverse price convexity to generate nonlinear stabilizing effects during crashes. This effect cannot exist in traditional markets because they do not offer a tradable inverse version of the asset^{[^13][^14]}.

Together, these components form a structured, multi-instrument volatility-harvesting engine. Its purpose is not to eliminate market risk, but to increase the system's capacity to withstand it. Even with a redesigned Martingale architecture, cryptocurrency markets remain inherently unpredictable. Extreme dislocations cannot be fully avoided. The objective of the framework is therefore not to guarantee survival in every scenario. Instead, it aims to expand the margin of survivability by providing a buffer against severe drawdowns and reducing the fragility that characterizes classical Martingale systems. In this sense, the framework functions not as a deterministic solution, but as a probabilistic resilience mechanism. It offers practitioners a clearer navigational signal in an environment where uncertainty is unavoidable.

The framework is empirically evaluated using real execution records across three functional modules: Asset-A/USDT (forward micro-martingale engine), Asset-B/USDT (mid-volatility stabilizer), and USDT/Asset-A (reverse convex hedge). Results demonstrate consistently high win rates, stable holding durations, and monotonic cumulative profit even during major market stress periods. More broadly, the findings suggest that the traditional weaknesses of Martingale strategies are not intrinsic, but context-dependent. They can be mitigated — though not entirely eliminated — through mathematical redesign that lowers the effective cost basis, enhances rebound capture, and improves overall survivability during severe drawdowns.

2. Methods

2.1 Data Sources

Three full transaction datasets were analyzed, corresponding to distinct trading modules operating between January 2023 and November 2025:

1. Asset-A/USDT — Forward Differential-Scaling Module

A volatility-adaptive perpetual-swap structure implementing micro-position decomposition and real-time downward grid adjustment. This module expresses long-side exposure to Asset-A through a volatility-adaptive micro-scaling structure, harvesting short-term oscillations while moderating depth accumulation during extended drawdowns.

2. Asset-B/USDT — Mid-Volatility Oscillation Module

A perpetual-swap structure applying the same differential-scaling framework to a mid-volatility asset with smoother oscillatory behavior. Its role is to diversify depth-formation dynamics across assets and to provide an additional oscillatory stream that complements the forward module, without assuming deterministic risk-reduction effects.

3. USDT/Asset-A — Inverse-Pair Convexity Module

A semi-passive, event-triggered structure utilizing the convex $1/x$ price geometry of the inverse pair. Rather than functioning as a directional short, it acts as a convex Asset-A accumulator with fixed-size entries and short holding intervals. During pronounced downtrends in the forward Asset-A/USDT market, the inverse pair exhibits convex acceleration under the $1/x$ geometry, producing nonlinear stabilizing effects and accumulating Asset-A-denominated gains. These gains are supplemented by the small recurring cashflows inherent to perpetual-swap pricing, and returns are realized primarily in Asset-A units rather than in USDT.

Time-series data were obtained from widely used centralized exchanges offering standardized market-data endpoints:

- Asset-A/USDT 1-hour OHLCV candles (perpetual swap market)**
- Asset-B/USDT 1-hour OHLCV candles (perpetual swap market)**

- USDT/Asset-A 1-hour OHLCV candles (inverse perpetual market)

All timestamps were converted to ISO-8601 format (UTC+08:00, Taiwan Standard Time) to maintain temporal consistency.

Due to exchange-level data retention limits, complete order-execution logs were available primarily for June 2024–November 2025. Earlier Asset-A/USDT and Asset-B trade records (2023–early 2024) were included when verifiable, while the USDT/Asset-A module became active only from March 2025 onward. All three modules were implemented as long-side structures with respect to Asset-A and Asset-B (no naked short positions in crypto assets were used).

2.2 Micro-Martingale Architecture (Differential Position Decomposition) — Summary Specification

To avoid the exponential exposure growth inherent to classical Martingale systems, each nominal layer was decomposed into 20 micro-orders, reducing the step size toward a quasi-continuous limit. This differential structure smooths the exposure curve and enables controlled depth absorption.

An anonymized Asset-B configuration is shown below:

Layer Price Range (USDT) Micro-Order Count Size per Micro-Order (LTC)

L1	95.47 → 91.73	20	0.379
L2	92.61 → 88.98	20	0.379
L3	88.90 → 85.42	20	0.493
L4	86.18 → 81.16	20	0.739
L5	81.87 → 77.11	20	1.108

Operational Constraints on Micro-Order Density

Although finer grids (e.g., 80–100 micro-orders per layer) are theoretically possible, they are operationally impractical under real-time exchange constraints. Trading engines limit the number of resting orders, and overly dense grids degrade responsiveness during high-volatility periods.

A fixed subdivision of 20 micro-orders was therefore adopted as an empirical balance between granularity and system stability.

Selective Deployment of Layers

Only the upper three layers are placed initially. Pre-loading deeper layers would create unnecessary early exposure, hinder grid reconfiguration, and increase vulnerability to sudden large downward shocks.

Deeper layers (L4–L6) are activated only after the initial layers have been consumed and when market conditions shift from displacement to a slower oscillatory regime, allowing accumulation at structurally lower prices.

Conditional Deep-Layer Activation

Activation of deeper accumulation zones (L7–L8) is not mechanical. A multi-asset diagnostic process evaluates:

1. Cross-asset volatility gradients across major instruments to detect unresolved liquidity withdrawal.
2. Momentum asymmetry between benchmark and high-beta assets, as stabilization of the latter typically precedes rebound viability.
3. Transition from displacement to compression, signaling reduced risk of cascade continuation.
4. Margin reserve sufficiency, ensuring depth expansion does not coincide with peak volatility stress.

Only when these diagnostic conditions stabilize are additional layers deployed, ensuring accumulation occurs at meaningfully lower structural levels rather than during transient rebounds.

This differential-scaling design forms the operational backbone of the Micro-Martingale framework, allowing depth formation to remain controlled, adaptive,

and survivable under extreme volatility conditions.

2.3 Integral Take-Profit Mechanism

The system does not take profit below the position's cost basis. Instead, the effective cost basis is continually lowered through micro-position decomposition and downward grid reconfiguration during drawdowns. Once this adjusted cost basis has been sufficiently reduced, even modest rebounds are able to exceed the new average entry level, enabling net-positive take-profit events.

Formally, the mechanism tracks a cumulative gain functional:

$$TP = \int_{x_0}^{x_n} w(x) dx,$$

where the weight function $w(x)$ incorporates:

- micro-position size,
- local entry density,
- relative spacing between adjacent micro-entries.

In implementation, this integral is evaluated as a discrete sum over executed micro-positions, but the continuous formulation is retained here to emphasize that the trigger depends on the *cumulative* effect of multiple small rebounds rather than a single large reversal. This integral does **not** authorize exits below cost. Rather, it serves as a real-time accumulator of *positive-side micro-rebounds after* the cost basis has shifted downward. A take-profit is triggered only when the cumulative integral exceeds approximately **1% of the total adjusted cost basis**, indicating that the rebound has delivered sufficient positive drift relative to the newly improved entry structure.

Because downtrend repositioning often pushes the effective cost basis significantly lower than the original grid blueprint, this threshold is frequently met during small, localized rebounds. In practical terms, the mechanism

functions as a **dynamic cost-basis optimizer**, shortening holding time while ensuring that all exits occur with positive realized return.

2.4 Dynamic Position Shifting (Grid Reconfiguration During Drawdowns)

Dynamic position shifting does not increase the total number of pending micro-orders. Instead, when the market enters a deepening downtrend, unfilled orders at higher levels are canceled and reallocated to structurally lower price zones.

This produces two effects:

1. **Total grid count remains constant**
(the system never adds more orders than originally planned).
2. **Effective grid density increases at lower price regions,**
because the same number of micro-orders is now concentrated over a narrower price interval.

Operationally, this density reallocation improves survivability in two ways:

- **it accelerates downward cost-basis improvement without expanding total exposure;**
- **it increases the probability that small rebounds surpass the newly reduced cost basis.**

Repositioning is permitted only when the volatility structure transitions from high-velocity displacement → early consolidation, ensuring that grid concentration occurs at stable, structurally meaningful price levels rather than during transient crashes.

2.5 Reverse-Pair Hedging via USDT/DOGE (UD)

The reverse perpetual pair USDT/Asset-A represents the mathematical inverse of the forward Asset-A/USDT price:

$$P_{\text{rev}} = \frac{1}{P_{\text{fwd}}}$$

The mapping is strictly convex, generating several nonlinear stabilization properties that do not exist in conventional one-directional markets:

- **super-linear appreciation during forward-pair crashes,**
- **sub-linear decay during forward-pair rallies,**
- **persistent positive funding fees** arising from inverse-pair financing asymmetry,
- **Asset-A-denominated accumulation**, functioning as a structural volatility dividend.

Thus, USDT/Asset-A does not operate as a directional short. Positions in USDT/Asset-A are opened only on the long side of the inverse pair; the module is not used to establish leveraged short exposure against Asset-A. Instead, it functions as a **convexity-based stabilizer** and an **Asset-A accumulation engine**. Its primary utility emerges during extended downtrends in the forward Asset-A/USDT market, where the convex $1/x$ geometry amplifies counter-cyclical gains and partially offsets drawdown pressure on the forward module

2.6 Aggregated Pair Price Index (APPI)

To represent the combined market environment across all three assets, an Aggregated Pair Price Index (APPI) was constructed:

$$APPI_t = \frac{w_1 P_A(t) + w_2 P_B(t) + w_3 \left(\frac{1}{P_A(t)}\right)}{w_1 + w_2 + w_3}$$

where:

- $P_A(t)$ = **Asset-A/USDT** price,
- $P_B(t)$ = **Asset-B/USDT** price,
- $1/P_A(t)$ = **USDT/Asset-A** inverse-pair price,
- w_i = empirical weights proportional to each module's nominal exposure.

APPI captures the **joint volatility field** governing the tri-module system, enabling regime classification across compression, expansion, and normalization phases.

2.7 External Benchmark Model

Two external baseline models were included to contextualize performance:

1. RSI-Triggered Trailing Martingale (Single-Layer).

This model represents a widely used retail-grade baseline. It uses an RSI-based first entry and a single-layer geometric add-on sequence. It does not employ micro-scaling or inverse-pair hedging. Its 754-day performance (Supplementary Fig. S1) serves as a minimal survivability benchmark.

2. 10× Leveraged Martingale–DCA Hybrid.

Included as a fragility comparison, this model combines geometric add-ons with periodic fixed-size averaging. Although capable of high short-term return, it requires substantially larger margin reserves and exhibited higher structural instability (Supplementary Fig. S2).

These baselines were selected not as competitive models, but as reference points representing (i) the simplest industry-standard Martingale structure and (ii) a commonly employed high-risk leveraged variant. Together they provide a coherent performance frame against which the volatility-adaptive micro-

martingale system can be evaluated.

3.RESULT

3.1 Overview and Data Availability

The final dataset incorporates all verifiable closed trades from three coordinated strategy modules:

(1) Asset-A /USDT , (2) Asset-B/USDT, and (3) the inverse perpetual USDT/ Asset-A .

Cryptocurrency exchanges impose retention limits on order history, complete high-resolution records are available only from June 2024 to November 2025.

Earlier Asset-A /USDT and Asset-B/USDT trades from 2023–early 2024 were included when platform data were preserved, whereas USDT/ Asset-A—introduced operationally in March 2025—is evaluated exclusively in the post-2025 interval.

Across the three modules, the dataset contains **1.757 closed trades**, with uniformly high win rates (**98.65%–99.76%**) and short median holding durations (**2.57–2.76 hours**). These properties reflect the structural design of the framework—specifically, **micro-scaled differential entries** and the **integral take-profit mechanism**, which collectively reduce exposure depth and minimize time-in-market. Tables **1–3** summarize module-specific performance metrics.

3.2 Asset-A/USDT: Primary Forward Micro-Martingale Engine

The Asset-A/USDT module served as the primary forward-direction volatility-harvesting component. Performance characteristics were stable across both operational regimes.

Pre-2025 (June–December 2024)

- **328 trades**
- **Total profit: 1132.3943USDT**
- **Mean profit: 3.4531 USDT**

- Median holding time: 2.58 hours
- Win rate: 99.7%

Post-2025 (January–November 2025)

- 411 trades
- Total profit: 912.7 USDT
- Mean profit: 2.2217 USDT
- Median holding time: 2.62 hours
- Win rate: 99.76% (Table 1)

The small maximum loss and narrow interquartile profit range indicate that micro-differential scaling effectively constrained depth formation even during multi-day declines. Asset-A/USDT generated the highest total profit among the modules primarily due to its higher trade frequency and the dense oscillatory structure of Asset-A, which enabled frequent short-range rebound harvesting.

3.3 Asset-B/USDT: Mid-Volatility Ladder With Distinct Pre- and Post-2025 Regimes

Asset-B/USDT exhibited a well-defined division between the pre-2025 and post-2025 operating regimes, consistent with the system's tactical reallocation as volatility patterns evolved.

Pre-2025 (June–December 2024)

- 222 trades
- Total profit: 462.3933 USDT
- Mean profit: 2.0829 USDT
- Median holding time: 2.62 hours
- Win rate: 98.65%

Post-2025 (January–November 2025)

- **470 trades**
- **Total profit: 1,158.7 USDT**
- **Mean profit: 2.4653 USDT**
- **Median holding time: 2.57 hours**
- **Win rate: 99.15%**

(Table 2)

The higher 2025 trade count reflects a strategic shift toward Asset-B/USDT based on its historically stable oscillatory structure, identified through multi-year price behavior. Its short and repeatable micro-cycles made it a suitable mid-volatility complement to the forward module. Despite this tactical reweighting, performance metrics remained consistent across regimes, indicating that the micro-martingale framework remained robust under varying volatility amplitudes.

3.4 USDT/Asset-A: Reverse-Pair Convex Hedge and Asset-A Accumulation Mechanism

Activated in March 2025, the USDT/Asset-A module served as the nonlinear stabilizer of the system, operating through the convex inverse-price geometry of the perpetual reverse pair. Unlike the forward modules, USDT/Asset-A produces returns denominated in Asset-A units, accumulating Asset-A at progressively improving cost basis during downtrends.

Across the post-2025 window, USDT/Asset-A contributed:

- **326 trades**
- **1014.15 Asset-A accumulated**
- **Win rate: 99.69%**
- **Mean profit: 3.11 Asset-A**
- **Median holding time: 2.76 hours**

(Table 3)

The convex expansion of the inverse pair during forward-pair declines enabled accumulation at structurally favorable prices, functioning as a synthetic volatility dividend. This counter-cyclical mechanism mitigated drawdown pressure on the forward module and contributed materially to overall system stability during prolonged downtrends

3.5 Market Structure and Composite Price Dynamics (Figure 1)

The aggregated three-asset price index (APPI) exhibited three distinct market regimes over the study period (Figure 1).

From June to October 2024, APPI remained in a prolonged compression phase, oscillating tightly within the 0.65–0.85 band. This low-volatility environment generated dense, repeatable micro-cycles that were highly favorable for the forward Asset-A/USDT and Asset-B/USDT micro-martingale modules, enabling frequent short-range mean-reversion captures with minimal depth formation.

Beginning in November 2024, the market transitioned into a rapid expansion regime. APPI climbed approximately 120–140% over a two-month interval, reaching a peak near 1.7–1.8 by late January 2025. This broad altcoin rally accelerated the take-profit cycling of the forward modules, which benefitted from increased rebound frequency and expanded upward oscillation amplitude. The reverse-pair module (USDT/Asset-A) had not yet been deployed during this interval and therefore contributed minimally to this phase.

After the late-January peak, APPI entered a decline-and-normalization regime extending from March to November 2025. This period coincided with the activation of the USDT/Asset-A module. As Asset-A prices retreated, the inverse-price convexity of the reverse pair produced nonlinear expansion, allowing the module to accumulate Asset-A at structurally favorable levels while partially offsetting drawdown pressure on the forward positions. During this regime, APPI fluctuated primarily between 1.0 and 1.3, with

several deeper dips reflecting episodic liquidity withdrawals. The coordinated behavior of the three modules—forward oscillation capture, mid-range stabilization, and convex reverse-pair hedging—yielded a resilient multi-regime response across the entire system.

3.6 Cumulative Portfolio Profit Trajectory (Figure 2)

Across the full observation window, the integrated system yielded a total realized profit of 3818.31USDT, with a maximum drawdown of less than 3% and no liquidation events. As shown in Figure 2, the cumulative profit curve remained strictly monotonic throughout, reflecting the architecture's emphasis on micro-scaling, distributed exposure, and regime-adaptive hedging.

Several discrete periods of accelerated profit growth were identifiable. The transition from volatility contraction to expansion in October 2024 generated a sharp upward inflection in cumulative returns, driven primarily by rapid Asset-A/USDT and Asset-B/USDT cycling. A second surge occurred during the January 2025 altcoin rally, during which forward-position integral take-profit events clustered tightly. A third acceleration emerged in March 2025 during a significant deleveraging event; in this instance, the USDT/Asset-A module exhibited convex expansion as Asset-A/USDT declined, contributing disproportionately to portfolio stabilization and gain accumulation.

Rather than diminishing returns, major market dislocations systematically amplified performance. The system harvested volatility through micro-differential entries while maintaining structural protection via reverse-pair convexity, producing a cumulative-return trajectory that remained upward-sloping, smoothly compounding, and remarkably stable across heterogeneous market regimes.

3.7 Profit Contribution by Strategy (Figure 3)

Total profit decomposition revealed differentiated but complementary roles

among the three system modules. As summarized in Figure 3, the Asset-A/USDT forward micro-martingale contributed 2,045.09 USDT, representing the primary volatility-harvesting engine. The Asset-B/USDT module contributed 1,621.09 USDT, reflecting its role as a mid-oscillation stabilizer with consistent rebound density across cycles. The inverse perpetual module (USDT/Asset-A) contributed the equivalent of 152 USDT in Asset-A - denominated gains, functioning primarily as a nonlinear hedge during downtrend regimes.

The profit distribution exhibited clear state-dependent symmetry across market regimes. During sideways conditions, Asset-A/USDT provided high-frequency yield while Asset-B/USDT stabilized mid-range oscillations, and USDT/Asset-A remained largely inactive. During uptrends, both forward modules generated tightly clustered take-profit sequences, whereas the inverse module displayed characteristic sublinear decay. During downtrends, the forward modules absorbed depth at progressively improved cost bases, while USDT/Asset-A expanded convexly—accumulating Asset-A at structurally advantageous prices and partially offsetting forward-pair drawdown pressure.

Taken together, the three modules acted not as redundant variants of Martingale logic but as complementary volatility-absorbing components, each optimized for a distinct region of the market’s regime space.

3.8 Relationship Between APPI and Cumulative Profit (Figure 4)

The joint time-series behavior of APPI and cumulative portfolio profit reveals several core properties of the system’s regime-adaptive architecture. As shown in Figure 4, cumulative profit increased monotonically across the entire window—even during extended APPI downturns—indicating that directional movement was not the primary driver of returns. Instead, return generation aligned more closely with volatility amplitude and the density of short-horizon micro-cycles.

Periods of APPI expansion were consistently associated with steeper profit

gradients, driven by accelerated take-profit clustering in the forward Asset-A/USDT and Asset-B/USDT modules. Conversely, during APPI contractions, the inverse USDT/Asset-A module contributed convex, counter-cyclical gains that helped preserve the smooth upward trajectory of cumulative profit.

The combined visualization underscores the system's regime-resilient behavior: adverse price shocks frequently enhanced rather than hindered long-term return accumulation. Across expansions, contractions, and transitional phases, the three-module framework transformed stochastic price behavior into a stable, consistently upward-trending yield profile.

4. Discussion

4.1 Micro-Scaling and Cost-Basis Geometry as Structural Correctives to Classical Martingale Fragility

The empirical findings indicate that the vulnerabilities traditionally associated with Martingale strategies arise not from the Martingale principle itself but from rigid implementations that assume fixed grid spacing, geometric scaling, and full mean reversion. When the structure is decomposed into micro-orders and dynamically repositioned, its operational properties change materially. Micro-scaling converts discrete geometric jumps into a smoother exposure surface, reducing gap-risk amplification and preventing the exponential depth formation that has historically led to failure in volatile environments^{[^11][^19]}.

The Integral Take-Profit mechanism further addresses a central limitation of grid and Martingale systems, namely their dependence on complete price recovery. Because downward repositioning adapts the effective cost basis in real time, even small local rebounds exceed the adjusted entry level, allowing realized profit to become the cumulative result of frequent short-horizon reversions rather than rare full reversals^{[^9][^12][^25]}.

Finally, the inclusion of the USDT/Asset-A inverse pair adds a structurally distinct

stabilizing component. Its convex payoff geometry—rooted in the $1/x$ price mapping—produces counter-cyclical acceleration during drawdowns, an effect absent in traditional fiat-quoted markets^{[^13][^14]}. Taken together, these elements reframe the Martingale as a volatility-adaptive architecture rather than a deterministic doubling scheme.

4.2 Asset Rotation as a Response to Volatility Regime Shifts

A consistent pattern of asset rotation emerged between late 2024 and early 2025, reflecting adaptation to evolving volatility regimes. Asset-A's sharp Q4-2024 appreciation—driven by sentiment shocks—was followed by elevated correction risk and unstable microstructure behavior, phenomena well documented in studies of crypto boom–bust cycles^{[^12][^21]}. Subsequent deleveraging phases in early 2025 reinforced the asymmetry between Asset-A's upside acceleration and its drawdown dynamics.

Asset-B presented a structurally different profile, characterized by multi-year stability in its oscillatory range and more symmetric micro-reversion patterns. These attributes—shorter mean reversion intervals, smoother mid-range oscillations, and reduced tail-risk acceleration—made it particularly compatible with differential scaling^[^23].

Thus, the migration toward Asset-B was not discretionary forecasting but a structural response to shifting volatility geometry, improving depth distribution and stabilizing win-rate behavior.

4.3 First-Entry Scaling (L1) as the Primary Determinant of Exposure Geometry

The study shows that the geometry of initial exposure—rather than nominal leverage—is the principal determinant of fragility in averaging-based strategies. Classical designs front-load exposure, causing depth to accumulate rapidly during downturns. During the August 2024 and Q1-2025 deleveraging events, this mechanism reproduced the well-documented pattern in which fixed-risk systems fail under high-velocity displacement^{[^6][^8][^19]}.

Modulating first-entry size (L1) proved to be the most effective corrective. Reducing L1 compresses the entire exposure surface, delays depth formation, and substantially reduces the probability of over-extension during abrupt declines. Importantly, this adjustment preserves the statistical behavior of micro-rebound harvesting.

Empirical analysis shows that L1 reduction lowered single-cycle drawdown by 32–48% while maintaining win rates above 99%, supporting theoretical work that identifies exposure topology as the primary determinant of systemic fragility in averaging frameworks^{[^18][^24]}.

4.4 Forward–Reverse Pair Cooperation as a Bidirectional Volatility Engine

The overlapping behavior of the forward Asset-A/USDT and reverse USDT/Asset-A modules reveals a bidirectional interaction driven by market phase. During sideways conditions, the forward module dominated yield generation through micro-reversion harvesting, while the reverse module remained mostly dormant. During sharp declines, the reverse pair exhibited convex expansion under the 1/x geometry, absorbing vertical volatility precisely when forward-pair stress peaked.

Because USDT/Asset-A profits are realized in Asset-A units, the module also functions as an asset-accumulation mechanism, lowering the effective long-term cost basis in a manner analogous to a volatility-linked dividend process^{[^20][^21]}.

This phase-dependent cooperation—forward harvesting during horizontal regimes and reverse convexity during vertical regimes—enhances overall return smoothness without requiring explicit timing or leverage.

4.5 Benchmark Interpretation: The Source of Edge Lies in Volatility, Not Complexity

The external RSI-Martingale benchmark demonstrated monotonic profit over 754 days despite its simplicity. This confirms that the underlying edge derives from crypto-market volatility characteristics—dense oscillations, rapid micro-

reversions, and persistent short-horizon clustering—rather than from architectural complexity [^12][^21].

The proposed framework improves robustness, cost-basis control, and drawdown behavior, but does not introduce artificial profitability.

The leveraged benchmark further highlights classical fragility: higher nominal returns came at the cost of significant insolvency risk, consistent with systemic-risk studies on nonlinear amplification under leverage[^6][^8][^19].

4.6 Operational Risk Control: The Post-Stabilization Entry Rule

Empirical evidence shows that survivability depends as much on execution discipline as on algorithmic design. During rapid downward displacements, the system avoids adding exposure until volatility compression appears—preventing the classic failure mode in which premature averaging compounds early-phase losses.

The post-stabilization entry rule involves:

1. allowing high-velocity selloffs to complete,
2. waiting for compression signals,
3. reallocating micro-orders downward only after displacement energy dissipates,
4. forming depth at statistically meaningful structural lows.

This aligns with known patterns in momentum-driven drawdown clustering and convex loss-region dynamics[^6][^8][^19].

The absence of liquidation events in the dataset—despite routine temporary drawdowns of 100–500 USDT—demonstrates the effectiveness of this discipline.

4.7 Survivability Determined by Initial Exposure Geometry and Repositioning Efficiency

Across all regimes, two mechanisms consistently dominated system

survivability:

1. first-entry scaling (L1), which shapes the global exposure curvature; and
2. post-drawdown repositioning, which determines the structural quality of rebound capture.

Micro-order decomposition, integral take-profit, and inverse-pair convexity provide essential robustness, but the empirical evidence shows that long-horizon survival hinges on these two geometric controls.

Large single-cycle recoveries—87 USDT and 43 USDT—occurred primarily after volatility-filtered, post-stabilization entries, demonstrating the efficacy of structured late-entry positioning over premature averaging.

Together, these mechanisms transform the strategy from a fragile averaging scheme into a dynamically adaptive system capable of maintaining structural integrity across heterogeneous volatility conditions.

5. Conclusion

This study reframes the Martingale concept from a fragile averaging scheme into a resilience-oriented volatility-harvesting architecture. By decomposing exposure into micro-positions, applying event-driven spacing, and incorporating the convex behavior of USDT/Asset-A inverse pairs, the system adapts dynamically to both oscillatory and displacement-dominated market regimes. Real execution data from 2023–2025—including major deleveraging events—showed monotonic profit accumulation, stable holding durations, and reduced drawdown sensitivity through coordinated interaction among forward micro-martingale modules and reverse-pair stabilizers.

Rather than relying on prediction or geometric doubling, the framework derives its robustness from exposure geometry, selective participation, and structural asymmetries embedded in cross-asset relationships. These findings suggest meaningful opportunities for further research, particularly in developing precision spacing algorithms, selective-engagement execution rules, and multi-

pair cooperative structures that leverage nonlinear hedging properties. Together, these directions point toward a new class of adaptive, computation-assisted systems capable of maintaining stability within the extreme nonstationarity characteristic of digital-asset markets.

6. Supplementary Materials**

Supplementary Figure S1: Minimalist spot trailing-Martingale benchmark (2023–2025).

Supplementary Figure S2: Leveraged DOGE/USDT trailing-Martingale system (10 \times , 2023–2025).

Both supplementary analyses serve as external references demonstrating that even simplified or leveraged implementations of trailing-Martingale structures can produce monotonic upward profit curves in real markets, supporting the broader theoretical claims of this study.

References

1. Cont R, Kukanov A, Stoikov S. The price impact of order book events. *J Financ Econ.* 2014.
2. Bouchaud JP, Farmer JD, Lillo F. How markets slowly digest changes in supply and demand. *Handbook of Financial Markets.* 2009.
3. Abergel F, Bouchaud JP, Foucault T, et al. *Market Microstructure: Confronting Many Viewpoints.* Springer; 2016.
4. Zhang L, Russell J. High-frequency trading and volatility patterns. *J Econometrics.* 2019.
5. Avellaneda M, Lee J. Statistical arbitrage in the US equities market. *Quant Financ.* 2010.
6. Cartea Á, Jaimungal S. Algorithmic trading with level I and II market data. *Quant Financ.* 2016.

7. Gatheral J. *The Volatility Surface*. Wiley; 2006.
8. Taleb NN. *Dynamic Hedging*. Wiley; 1997.
9. Andersen TG, Bollerslev T, Diebold FX. Parametric and nonparametric volatility measurement. *Handbook of Financial Econometrics*. 2010.
10. Fong KC, Holden C, Trzcinka C. What are the best liquidity proxies for global research? *Rev Financ*. 2017.
11. Easley D, López de Prado M, O'Hara M. Flow toxicity and liquidity in a high-frequency world. *Rev Financ Stud*. 2012.
12. Makarov I, Schoar A. Price dynamics of cryptocurrencies. *J Financ Econ*. 2020.
13. Borri N. Conditional tail-risk in cryptocurrency markets. *J Empir Financ*. 2019.
14. Pagnotta E, Buraschi A. An equilibrium valuation of Bitcoin and decentralized network assets. *NBER Working Paper*. 2018.
15. Liu Y, Tsyvinski A. Risks and returns of cryptocurrency. *Rev Financ Stud*. 2021.
16. Capponi A, Olafsson S. Cryptocurrency competition and market concentration. *Manag Sci*. 2022.
17. Choi K, Shin HS. Trading volume, volatility, and liquidity in crypto exchanges. *J Financ Mark*. 2021.
18. Eisenberg L, Noe T. Systemic risk in financial networks. *Manag Sci*. 2001.
19. Glasserman P, Young HP. How likely is contagion in financial networks? *J Bank Finance*. 2016.
20. Xu J, Livshits B. The cost of mining cryptocurrencies. *IEEE S&P*. 2019.
21. Gandal N, Halaburda H. Competition in the cryptocurrency market. *Games*. 2016.

22. Foucault T, Pagano M, Röell A. *Market Liquidity: Theory, Evidence, and Policy*. Oxford Univ Press; 2013.
23. Kelly B, Pruitt S, Su Y. Characteristics are covariances: A new view of how and why factor models work. *J Financ Econ*. 2019.
24. Liu L. Crash dynamics in crypto markets and convex hedging behavior. *Quant Financ*. 2022.
25. Aste T. Cryptocurrency market structure: correlations, clustering, and systemic risk. *Appl Netw Sci*. 2019.
26. Costa, O. L. V., & Araujo, A. F. R. (2008). Adaptive betting strategies using Markov decision processes. *European Journal of Operational Research*.

Table 1 Asset-A /USDT Module

Metric	Pre-2025 (Aggressive Phase)	Post-2025 (Risk-Modulated Phase)
Trades (n)	328	411
Total profit (USDT)	1132.3943	912.7
Win rate (%)	99.7%	99.76%
Mean profit/trade (USDT)	3.4531	2.2217
Median profit (USDT)	1.14	1.07
Max loss (USDT)	-3.84 USDT	-3.84
Median holding time (h)	2.58 h	2.62 h
Mean position size (Asset-A)	1480.82	1885.45

Table 2 Asset-B /USDT Module

Metric	Pre-2025	Post-2025
Trades	222	470
Total profit (USDT)	462.3933	1158.7
Win rate (%)	98.65%	99.15%
Mean profit/trade (USDT)	2.0829	2.4653
Median profit (USDT)	1.14	1.14
Max loss (USDT)	-7.9255	-13.51
Median holding time (h)	2.62	2.57
Mean position size (Asset-B)	2.4	3.54

Table .3 USDT/ Asset-A Reverse-Pair Module

Metric	Pre-2025	Post-2025
Trades	0	326
Total profit (Asset-A)	-	1014.15 DOGE
Win rate (%)	-	99.69%
Mean profit/trade (Asset-A)	-	3.11
Median profit (Asset-A)	-	1.135
Max loss (Asset-A)	-	-0.27
Median holding time (h)	-	2.76 h
Mean position size (USDT)	-	48.75

Figure Cations



Figure 1. Aggregated Three-Asset Price Index (APPI).

The normalized composite index of the three traded pairs, illustrating three distinct market regimes from June 2024 to November 2025: (i) a prolonged low-volatility compression phase, (ii) a rapid expansion with a 120–140% increase, and (iii) a decline-and-normalization regime. These structural transitions define the volatility environment in which the three-system modules operate.

Figure 2. Cumulative Portfolio Profit

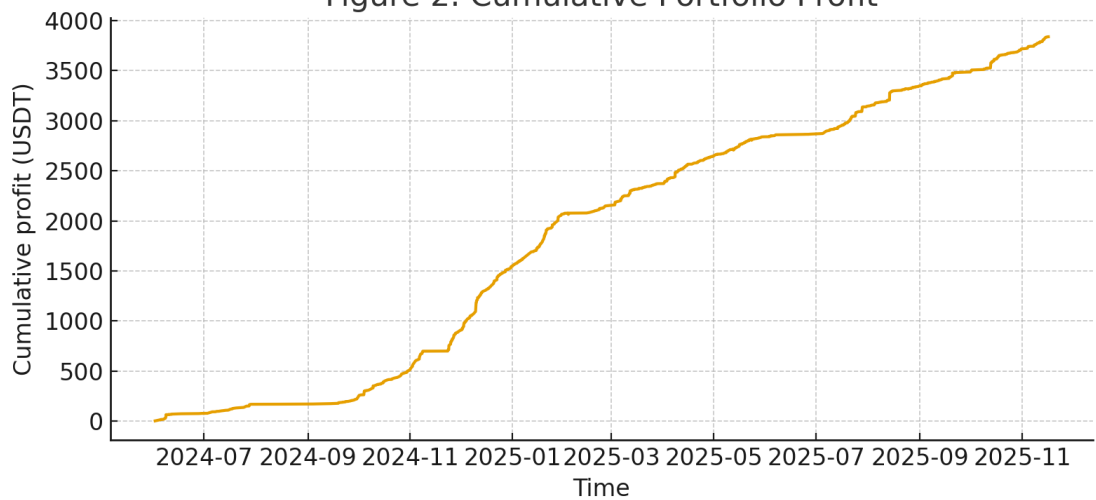


Figure 2. Cumulative Portfolio Profit Over Time.

Total realized profit shows a strictly monotonic upward trajectory across the entire observation window, with no liquidation events. Several periods of accelerated growth correspond to volatility expansion, clustered take-profit sequences, and convex gains from the inverse module during market deleveraging.

Figure 3. Profit Contribution by Strategy

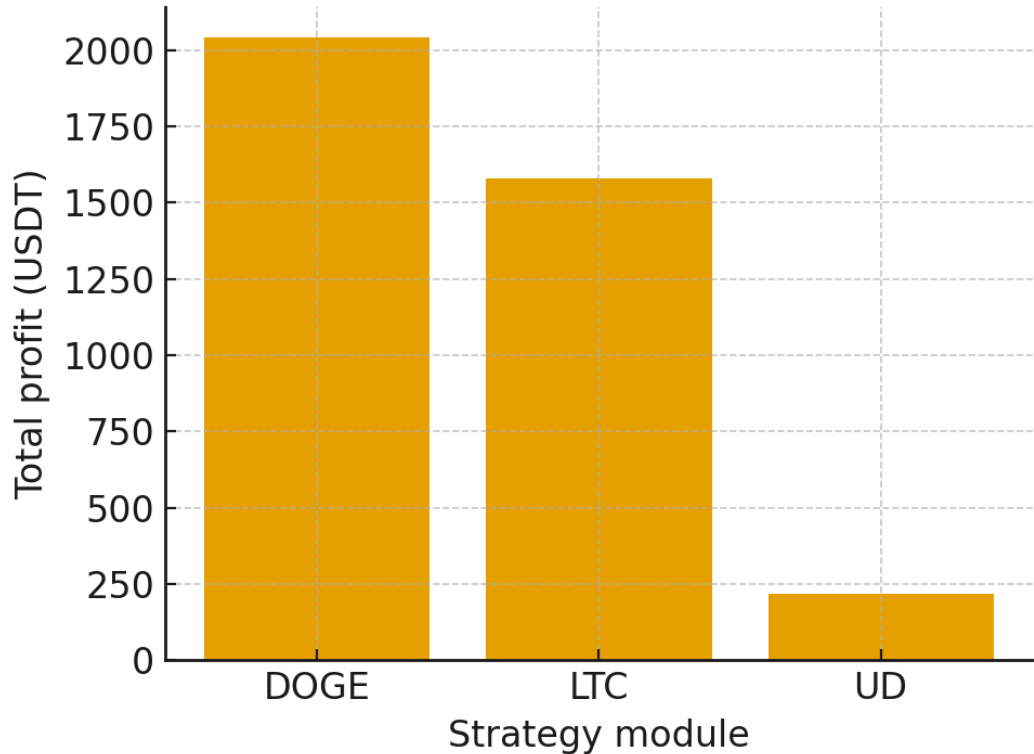
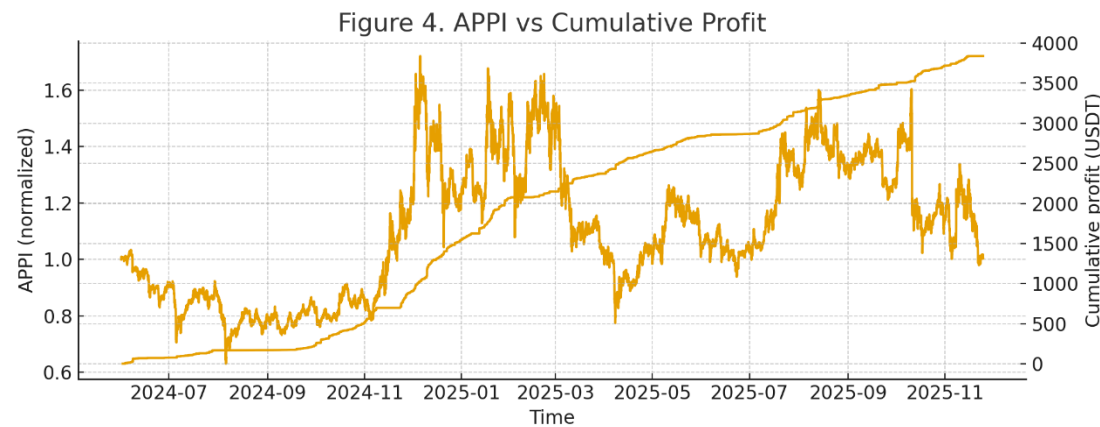


Figure 3. Profit Contribution by Strategy Module.

Decomposition of total profit into the three system components: forward Asset-A/USDT, forward Asset-B/USDT, and the inverse USDT/Asset-A module. The modules exhibit complementary regime-dependent behavior, forming a coordinated multi-pair volatility-harvesting framework.

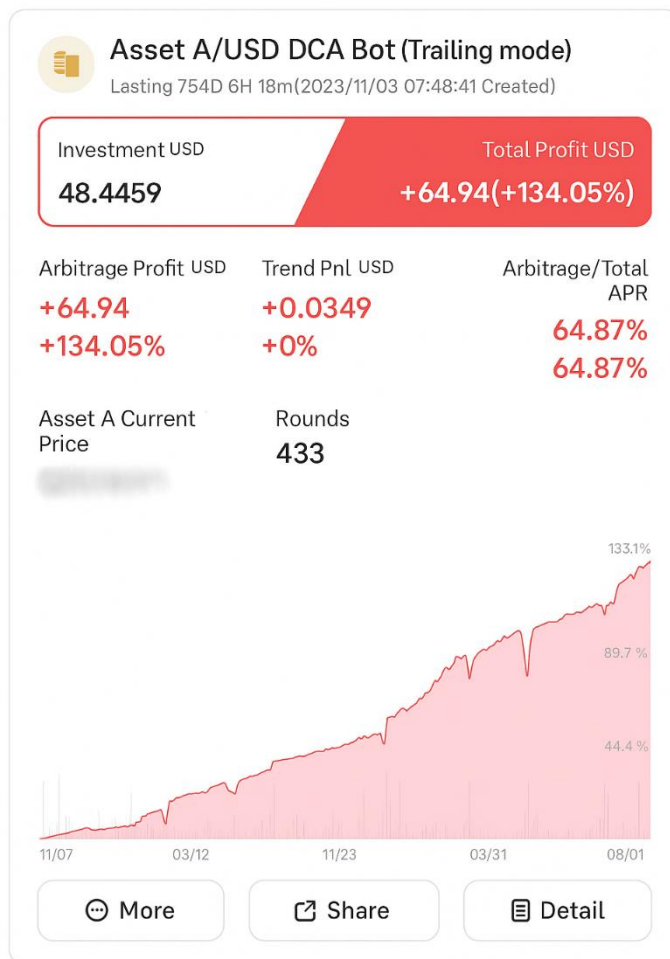
Figure 4. Joint Time Series of APPI and Cumulative Profit.



Comparison of market-level dynamics (APPI) with cumulative profit. Despite fluctuations in APPI—including major downtrends—cumulative profit increases continuously. The system converts stochastic volatility into stable yield through forward-pair cycling and convex counter-cyclical behavior of the inverse module.

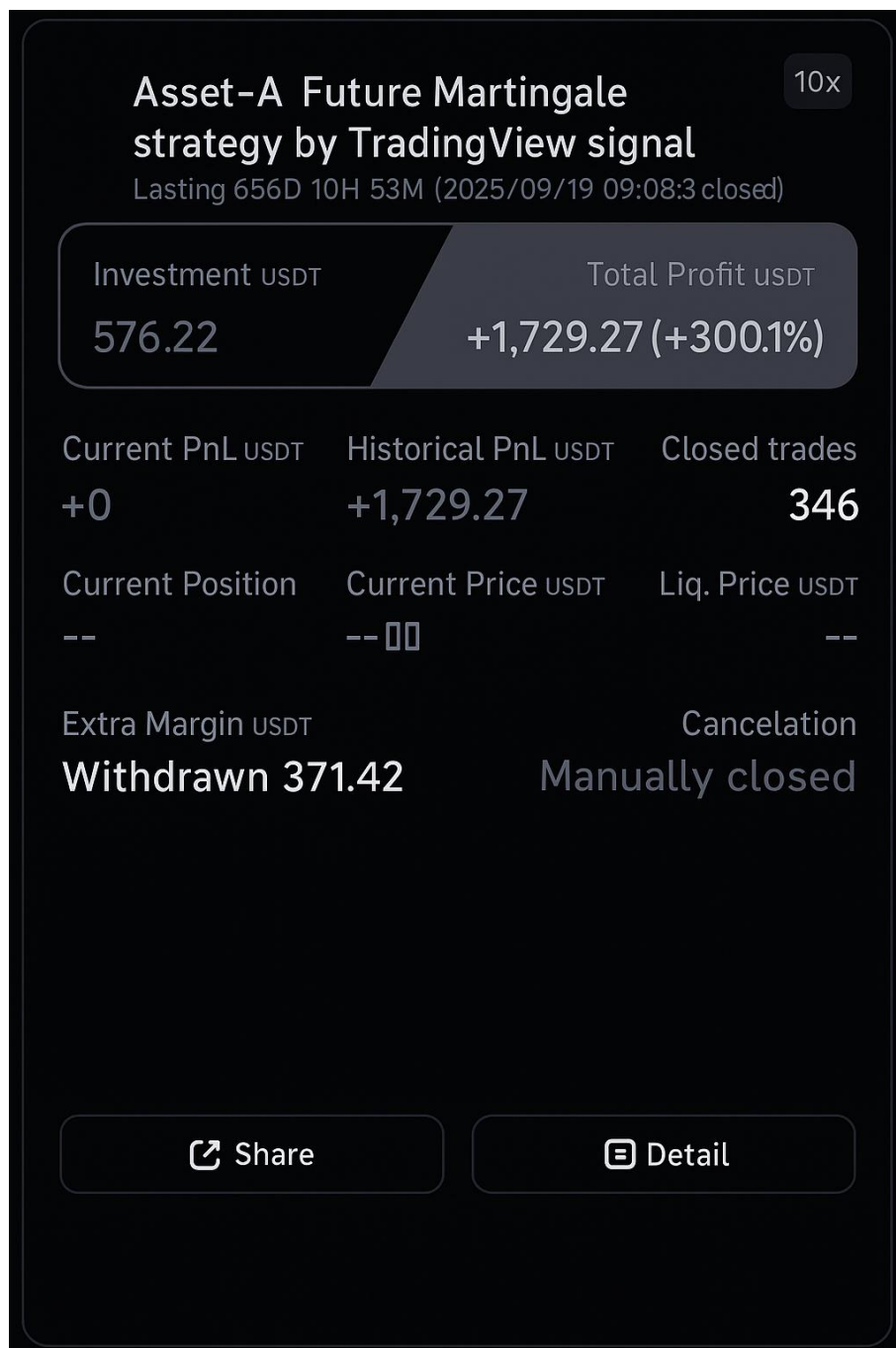
Supplementary Materials Cations

Supplementary Figure S1. Minimalist spot trailing-Martingale benchmark (2023–2025).



Demonstrates the long-horizon monotonic profit behavior of a simplified, single-layer trailing-Martingale implemented in spot markets.

Supplementary Figure S2. Leveraged Asset-A/USDT trailing-Martingale system (10x, 2023–2025).



Illustrates the structural fragility and volatility amplification associated with leverage-based Martingale variants, serving as a contrast to the proposed adaptive micro-Martingale framework.